On the application of forced Rayleigh light scattering to mass diffusion measurements

W. Urbach,[a] H. Hervet, and F. Rondelez
Physique de la Matière Condensée,[b] Collège de France, 11 Pl. Marcelin-Berthelot, 75231 Paris Cedex 05, France

(Received 27 December 1984; accepted 14 March 1985)

The newly developed forced Rayleigh light scattering (FRS) method has been applied to the measurement of anisotropic mass diffusion in well-aligned nematic samples of *p*-azoxy anisol (PAA) and *p*-methoxy benzilidene-*p*-*n*-butyl aniline (MBBA). Since both materials are photochromic and can thus be photochemically labeled, self-diffusion can be studied as well as impurity diffusion. In the latter case, the diffusing species was chosen to be methyl red (MR), which is photochromic but had also been used as a regular dye in optical tracer diffusion experiments. The FRS data for self-diffusion are shown to agree well with this earlier determination; a satisfactory result if one considers that MR and both PAA and MBBA have very similar molecular structures. They also agree to within 10% with the Franklin theory of self-diffusion in liquid crystals. On the other hand, the FRS measurements of impurity diffusion with photochemically labeled MR give diffusion coefficients that are considerably smaller. This discrepancy can, in principle, be explained through nonequilibrium thermodynamic considerations which show that the diffusion coefficient actually measured by FRS is different in the two cases of self- and impurity diffusion. However, the observed variation seems anomalously large. We tentatively suggest that photoactivated MR molecules tend to form aggregates, a problem apparently not encountered with photoexcited MBBA or PAA molecules. This demonstrates that, although FRS is undoubtedly a powerful technique to measure mass transport, the possibility of photoinduced spurious intermolecular interactions between the diffusing species must always be considered with care.

I. INTRODUCTION

It is now well established that mass diffusion in anisotropic liquid crystalline phases must be described by a second-rank tensor D. In the most common case where the molecules are rod-like, the principal axes of that tensor are the average direction **n** of the long molecular axis and its perpendicular. The corresponding diffusion coefficients are called $D_{\parallel}$ and $D_{\perp}$, respectively. Their ratio $D_{\parallel}/D_{\perp}$ is generally greater than unity in nematic phases and smaller than unity in smectic phases,[1] however, complications due to pretransitional fluctuations may arise in the vicinity of phase changes.[2]

Numerous experimental techniques have been put to use to study mass transport in nematic phases: tracers,[3–5] nuclear magnetic resonance,[6–8] and quasielastic neutron scattering.[9–10] The results can be roughly classified in two categories, self-diffusion or impurity diffusion, according as the diffusing species are the molecules of the matrix itself or externally added impurities. Quasielastic neutron scattering (QENS) data invariably belong to the first category, NMR the tracer data to either one depending on the particular experiment. Despite an increase in sophistication over the years, especially for NMR with the advent of the multiple pulse sequence spin-echo method[7] and for QENS with the availability of high resolution spectrometers at the high flux reactor in Grenoble,[10] all the above techniques have their drawbacks. It has been gradually recognized that many of the results in the early literature are erroneous.[11] As a consequence, a considerable sifting of the existing data is required even though the gross features of mass diffusion in liquid crystals are now qualitatively understood.

In view of this uncomfortable situation, we have developed a new method, called the forced Rayleigh light scattering (FRS), which allows the accurate determination of mass diffusion coefficients on the condition that the molecules are photoexcitable. It is particularly suited to anisotropic liquid crystalline phases since it only requires tiny monodomains and can be used to measure transport coefficients in any direction relative to the alignment axis. In two preceding reports, we have presented the main features of FRS and shown data in liquid crystals[12] and in solutions of flexible polymers.[13] In this paper, we present additional results on mass transport in the nematic phase of two extensively studied liquid crystalline materials, namely *p*-methoxy benzilidene-*p*-*n*-butyl aniline (MBBA for short) and *p*-*p*′-methoxy azoxy benzene, also called *p*-azoxy anisol (PAA). We investigate both self-diffusion of the MBBA and PAA molecules and also impurity diffusion of methyl red, an externally added photochromic dye. We start by showing theoretically, using nonequilibrium thermodynamics, how FRS should measure two different diffusion coefficients depending on whether the photoexcited molecules are the molecules forming the liquid crystalline phase (self-diffusion) or are externally added photochromic impurities (impurity diffusion). We describe the experimental setup in Sec. III, together with the method used to analyze the data. The FRS results are

[a] Lab. Biophysique (ERA No. 498) C.H.U. Cochin, 24 rue du Fb. St. Jacques, 75674 Paris Cedex 14, France.
[b] Equipe de Recherche Associée au C.N.R.S. (ERA No. 542).

 0021-9606/85/161877-11$02.10

presented in Sec. IV. The two sets of data for self- and impurity mass transport show striking variations which cannot be explained by trivial differences between the shapes of the diffusing molecules. The discrepancy is also too large to be easily explained by the theoretical differences between the self- and impurity diffusion coefficients. Comparing our results with those obtained by more classical methods, (tracers, NMR, quasielastic neutron scattering) we are led in Sec. V to emphasize the importance of controlling the intermolecular interactions between the photochemically labeled diffusing molecules. Finally, in Sec. VI, we compare our data for the two components of the mass diffusion tensor with theoretical estimates by Franklin and by Chu and Moroi, respectively.

II. THEORETICAL BACKGROUND

A. Forced Rayleigh scattering

The basic idea of FRS for measuring mass diffusivity is to create in the sample a periodic distribution of photochemically labeled molecules, and to monitor the subsequent relaxation of this perturbation towards uniform distribution. Taking the problem as one dimensional, the initial concentration of photolabeled molecules is written as

$$C(x,0) = C(0,0)\cos^2 qx, \tag{1}$$

where q is the wave vector of the perturbation.

At later times, this concentration $C(x,0)$ will relax exponentially[12] according to

$$C(x,t) = C(x,0)\exp(-t/\tau) \tag{2}$$

with

$$\tau^{-1} = Dq^2, \tag{3}$$

where D is the mass diffusion coefficient of the photolabeled molecules. It should be pointed out that this simple result is only valid for infinitely long-lived photoactivated species. If the intramolecular relaxation time τ_R becomes non-negligible compared to the mass diffusion time, the two contributions to the relaxation must be added. Therefore τ^{-1} becomes

$$\tau^{-1} = \tau_R^{-1} + Dq^2. \tag{4}$$

B. Isothermal diffusion in fluid mixtures

Mutual diffusion coefficients in condensed systems are generally measured by tracer techniques. This is not a limitation when the tagging is based on subtle nuclear modifications for a small fraction of the host molecules: protonation-deuteration for QENS, isotopic substitution for radioactive tracers, and perturbation of the Larmor frequencies of the nuclei in NMR. In such cases the labeled and the host molecules can be considered as identical species and the measurements yield the self-diffusion coefficient.

FRS, on the contrary, requires photoexcitable molecules which can have very different chemical structures between their ground and photoactivated states: *trans-cis* conformation changes with azobenzenes, heterolytic cleavage with benzo spiropyrans.[14] Moreover, if the medium is not photosensitive itself, it is then necessary to dissolve small amounts of a photochromic dye in the host phase. In both cases the measured diffusion coefficient may not reflect the true self-diffusion coefficient of the molecules of the matrix. In the following calculation, we will focus our attention on the chemical interactions between the various moieties of the mixture. The hydrodynamic interactions are supposed to be included in the mobility coefficients. We will first examine the equations of transport for a two-component system of molecules S and S^*, S^* being the photoactivated state of S. Then we will discuss three-component systems of solvent molecules S and of dye molecules A and A^*, A^* being the photoactivated state of A.

1. Two-component mixtures

In the most general case, we can write the free energy of the S–S^* binary mixture as[15]

$$F = kT(\Phi_S \ln \Phi_S + \Phi_S^* \ln \Phi_{S^*} + \chi \Phi_S \Phi_{S^*}). \tag{5}$$

Φ_S and Φ_{S^*} are the volume fractions of S and S^* and obey the additional incompressibility condition

$$\Phi_S + \Phi_{S^*} = 1. \tag{5'}$$

The interaction between the two species is described by the parameter χ. Positive values imply a tendency to segregation while negative values imply good solubility of S^* into S. The chemical potentials for each species are

$$\mu_S = kT(\ln \Phi_S + \chi \Phi_{S^*}) + \text{const},$$
$$\mu_{S^*} = kT(\ln \Phi_{S^*} + \chi \Phi_S) + \text{const}. \tag{6}$$

In irreversible thermodynamics, the currents (or fluxes) J's are related to forces by mobility coefficients Λ's. Therefore,

$$J_i = -\Lambda_i \nabla(\mu_i + U), \tag{7}$$

where $i = S$ or S^*. U is a potential introduced to impose the incompressibility of the system,[16] as described by Eq. (5'). U can be considered as an external pressure which maintains the system at constant volume. Setting $J_S + J_{S^*} = 0$ into Eq. (7) it is easy to show that

$$U = \frac{-(\Lambda_S \mu_S + \Lambda_{S^*} \mu_{S^*})}{\Lambda_S + \Lambda_{S^*}}. \tag{8}$$

Replacing U by its value in Eq. (7), J_{S^*} becomes

$$J_{S^*} = -J_S = -\frac{\Lambda_S \Lambda_{S^*}}{\Lambda_S + \Lambda_{S^*}} \nabla(\mu_{S^*} - \mu_S). \tag{9}$$

$\mu = \mu_{S^*} - \mu_S$ is the exchange chemical potential

$$\mu = \log \Phi_{S^*} - \log \Phi_S + \chi(\Phi_S - \Phi_{S^*}). \tag{10}$$

It is also possible to write J_{S^*} in terms of Φ_{S^*} alone,

$$J_{S^*} = -\frac{\Lambda_S \Lambda_{S^*}}{\Lambda_S + \Lambda_{S^*}} \left(\frac{1}{\Phi_{S^*}} + \frac{1}{1 - \Phi_{S^*}} - 2\chi \right) \nabla \Phi_{S^*}. \tag{11}$$

The mobilities Λ_S and Λ_{S^*} can alternatively be expressed in terms of the diffusion coefficients D_S^0 and $D_{S^*}^0$ at infinite dilution of S^*, defined by $J_i = -D_i^0 \nabla \Phi_i$ (with $i = S$ or S^*).

$$\Lambda_i = D_i^0 \Phi_i / kT. \tag{12}$$

Therefore, one gets

$$J_{S^*} = -\frac{D^0_{S^*}}{1-\Phi_{S^*}(1-D^0_{S^*}/D^0_S)} \times\left[1-2\chi\Phi_{S^*}(1-\Phi_{S^*})\right]\nabla\Phi_{S^*}. \quad (13)$$

For a two-component mixture, the mutual diffusion coefficient for S^* is defined by

$$J_{S^*} = -\tilde{D}^2_{S^*}\nabla\Phi_{S^*}. \quad (14)$$

Comparison between Eqs. (13) and (14), together with the condition $\Phi_{S^*} \ll 1$, yields the final result:

$$\tilde{D}^2_{S^*} = D^0_{S^*}\left[1+\Phi_{S^*}(1-2\chi-D^0_{S^*}/D^0_S)\right]. \quad (15)$$

If Φ_{S^*} decreases towards zero, $\tilde{D}^2_{S^*}$ goes to $D^0_{S^*}$ as expected in this limiting case.

2. Three-component mixtures

The case of three-component mixtures of solvent S plus dye molecules in their ground state A and their photoactivated state A^* is developed in detail in the Appendix. We will only point out the main results here.

The current of the $A^*(A)$ species can be expressed very generally as

$$J_{A^*} = -\tilde{D}_{A^*A^*}\nabla\Phi_{A^*} - \tilde{D}_{A^*A}\nabla\Phi_A. \quad (16)$$

To first order in Φ_A and Φ_{A^*}, and assuming $\Phi_S \simeq 1$, Eqs. (A6′) and (A10) yield

$$\left.\begin{aligned}\tilde{D}_{A^*A^*} &= D^0_{A^*}\left[1+\Phi_{A^*}(1-2\chi_{A^*S}-D^0_{A^*}/D^0_S)\right]\\ \tilde{D}_{A^*A} &= \Phi_{A^*}D^0_{A^*}\left[\chi_{AA^*}-\chi_{A^*S}-D^0_A/D^0_S\right]\end{aligned}\right\}, \quad (17)$$

where D^0_i is the mutual diffusion coefficient of the species i at infinite dilution of A (or A^*).

In the case of a FRS experiment, we have the supplementary condition that, following the writing pulse, $\nabla\Phi_A = -\nabla\Phi_{A^*}$. We can thus rewrite Eq. (16) as

$$J_{A^*} = -\tilde{D}^3_{A^*}\nabla\Phi_{A^*}. \quad (18)$$

The mutual diffusion for A^* in the three-component mixture is therefore

$$\tilde{D}^3_{A^*} \cong D^0_{A^*}\left[1+\Phi_{A^*}(1-\chi_{S^*S}-\chi_{AA^*} - D^0_{A^*}/D^0_S + D^0_A/D^0_S)\right]. \quad (19)$$

It is easy to check that if one returns to the two-component mixture by making $\nabla\Phi_A$ equal to zero and A^* identical to S^* in Eqs. (16) and (17), respectively, Eq. (19) simplifies into Eq. (15).

3. Application to our FRS experiments

Comparing the two- and the three-component cases described in Secs. II B 1 and II B 2, we come to the important theoretical conclusion that FRS measures different diffusion coefficients, depending on whether the photoexcitable molecules are the molecules of the solvent (binary diffusion, coefficient $\tilde{D}^2_{S^*}$) or are externally added molecules (ternary diffusion, coefficient $\tilde{D}^3_{S^*}$). Unfortunately, the theory does not allow for any prediction of the magnitude of the effect.

In general, one will try to choose a photochromic dye A which has a chemical structure as close as possible to that of the solvent molecules. Therefore one can reasonably assume that $D^0_A \cong D^0_S$. Moreover, if the photoactivated structure is not drastically different from that of the ground state one can also assume that $D^0_A \cong D^0_{A^*}$ (in ternary diffusion) and $D^0_S \cong D^0_{S^*}$ (in binary diffusion). With the above conditions, the main difference between $\tilde{D}^3_{A^*}$ and $\tilde{D}^2_{S^*}$ will arise from the interaction parameters χ_{ij}. Examination of Eqs. (19) and (15) shows that they come into play in a factor which also contains the volume fraction of photoactivated species Φ_{S^*} or Φ_{A^*}. At low excitation levels, these volume fractions are small, typically of the order of 10^{-3}. Since the χ_{ij} are of order of unity in general, the correction terms are weak and the diffusion measured by FRS in binary and ternary systems should be nearly identical in most practical cases. On the other hand, the $\chi_{ij}\Phi_i$ correction terms will be significant if the χ_{ij} are of order of 10^3. Such large values can only be found in pathological situations where there are special interactions, e.g., demixtion, between the components of the mixture, S and S^* or S, A, and A^*.

III. EXPERIMENTAL

The two components of the diffusion tensor, respectively parallel and perpendicular to the sample optical axis, have been measured at a single temperature in the nematic phase of MBBA and PAA. In both cases, two different sets of samples have been used: one containing the pure materials and the other containing, in addition, a low concentration (5×10^{-4} g/g) of methyl red (MR). MR was selected because its molecular structure is closely related to that of the host molecules (see Fig. 1).

Under ultraviolet photoexcitation, MBBA and MR ungergo a *trans* to *cis* isomerization around their azomethine or azo linkage, respectively.[14] In both cases, there is also a thermal (dark) process which converts the *cis* isomer back to the *trans* form. The dark reactions are activated processes characterized by an energy barrier. This barrier is generally higher, by a factor of the order of 2, for azobenzenes (e.g., MR) than for Schiff bases (e.g., MBBA). Therefore, the half-life of the *cis* state will be longer for MR than for MBBA. However,

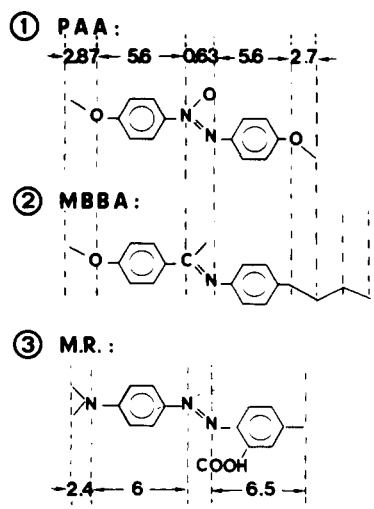

FIG. 1. Molecular structures of *p*-methoxy benzilidene *p*-*n*-butyl aniline (MBBA), methyl red (MR), and 4-4′ *p*-azoxy anisol (PAA). The numbers correspond to the lengths b_1 of the various segments projected onto the long molecular axis (values are in Å).

we will see in the following that illumination of *cis* MR in its visible absorption band can increase its return rate by one order of magnitude.

The photochromic properties of PAA are less clear-cut.[14] It is generally accepted that, on UV irradiation, azoxy compounds rearrange to *ortho*-hydroxy azo benzenes, the

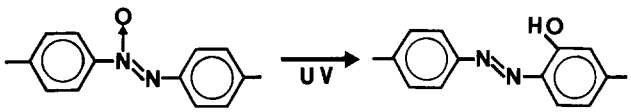

oxygen atom being transferred to the nonadjacent ring. This transformation is irreversible.

These structural changes are accompanied by modification in the optical properties. For example, it is well documented that the $II \rightarrow II^*$ electronic transition responsible for the UV absorption of azobenzenes around 350 nm shifts to lower wavelengths on conversion to the *cis* state, while there is a small increase in the strength of the $n \rightarrow II^*$ transition around 450 nm.[14] The forced Rayleigh method will be sensitive to these optical changes if they fall into a band which contains the wavelength at which the diffraction grating is observed. They will be detected whenever there is a variation in the imaginary part or in the real part of the complex refractive index of the photoactivated medium.[12,13]

The photoexcitation was performed with pulsed laser light at wavelengths corresponding to the absorption bands of the photoexcitable species. A cw argon laser was used at 350 nm for PAA and MBBA and at 514.5 nm for MR. Its output beam was chopped mechanically to produce short pulses of 40 μs (for MBBA or MR) and 400 μs (for PAA) duration with an adjustable repetition rate between 1 and 100 s. The light intensity incident on the sample was always kept as low as possible in order to avoid undesirable photolytic processes, while assuring reasonable signal-to-noise ratios. Its maximum value was 4×10^{-2} W for pure MBBA samples, 1.2 W for pure PAA samples, and 2×10^{-1} W for MR-doped PAA and MBBA samples.

The sinusoidal distribution of photoactivated species was achieved by splitting the laser beam in two equal parts and recombining them under a finite angle at the sample position. The periodic refractive index change (or absorption change) associated with this distribution creates a transient grating which diffracts the light issued from a continuous, low-power, He–Ne laser beam ($\lambda = 632.8$ nm). It was checked that in the case of MBBA and PAA, a 5 mW red illumination did not affect the relaxation time of the diffraction pattern. On the other hand, τ was observed to vary with the red incident power for MR-doped samples. This effect could be made negligible by lowering the He–Ne laser beam power to less than 5×10^{-7} W, discussed at length in Sec. IV. Figure 2 gives only a schematic representation of the experimental setup since a more detailed description can be found elsewhere.[12] The first diffracted order beam was collected on the photocathode of the phototube over less than one coherence area by using a 100 μm pinhole. In this case the output voltage of the phototube can be expressed in the form

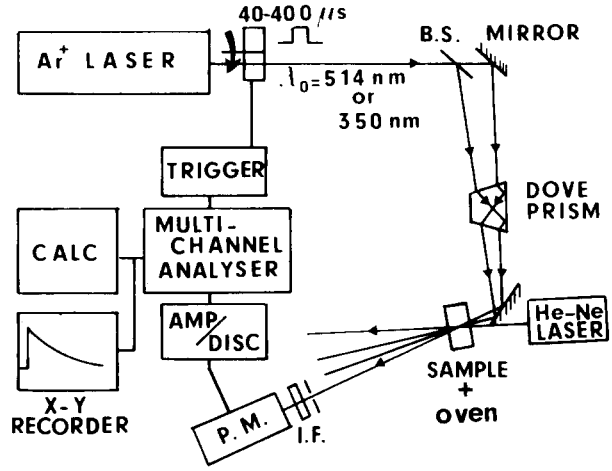

FIG. 2. Experimental setup. The exciting laser is a Spectra Physics model 165 Ar^+ laser capable of delivering 1.5 W at 514 nm or a Spectra Physics model 171 delivering 2 W at 350 nm. The fringe spacing can be adjusted by varying the angle between the two interfering beams. The mechanical chopper gives light pulses of 40–500 μs duration with a repetition time adjustable from 20×10^{-3} s to ∞. The diffracted intensity is collected with a radiotechnique-Compelec RTC-56 TVP photomultiplier. I.F. is an interference filter centered at 632 nm. The phototube output pulses are amplified and fed into a multichannel analyzer (Intertechnique BM 25) used in the multiscaler mode. The time dependence of the diffracted intensity is recorded after each exciting pulse and averaged over 10^3 pulses to improve the accuracy. The data are then processed with a Hewlett–Packard 9825 calculator.

$$V(t) = A\,(E_S e^{-t/\tau} + E_B)^2, \tag{20}$$

where E_S is the amplitude of the diffracted electromagnetic field. E_B is the amplitude of the time-independent scattered field due to static inhomogeneities and A is an amplitude factor.

The above equation assumes full spatial coherence between all scattered electromagnetic fields. If this condition holds true, then a slight shift of the phase of the local oscillator created by the static inhomogeneities relative to the diffracted electromagnetic field should change the shape of the detected signal if $E_B \gg E_S$ (heterodyne detection). This was indeed observed experimentally and the phase matching was achieved by maximizing the signal amplitude.

The experimental data are fitted to expression (20), using a nonlinear least-squares procedure.[17] Estimations of the fit goodness were calculated with the classical χ^2 criteria and the quality factor Q defined by Tournarie[18]:

$$Q = 1 - \sum_{i=1}^{N-1} \frac{\epsilon_i \epsilon_i + 1}{\epsilon_i^2}, \tag{21}$$

where ϵ_i is the experimental value of $V(t)$ minus the theoretical one.

Fits were accepted only if $\chi^2 \geqslant 0.98$ and $Q \geqslant 0.8$. Typical semilogarithmic plots of the phototube output voltage are shown in Fig. 3 for various power levels of the pulsed excitation in the case of a MBBA sample doped with MR. The relaxation time τ can be directly deduced from the slope of the linear part of the curve. For large exciting powers, there is evidence of nonlinearity at initial times. Such data, which are probably related to spurious photochemical reactions, were systematically discarded.

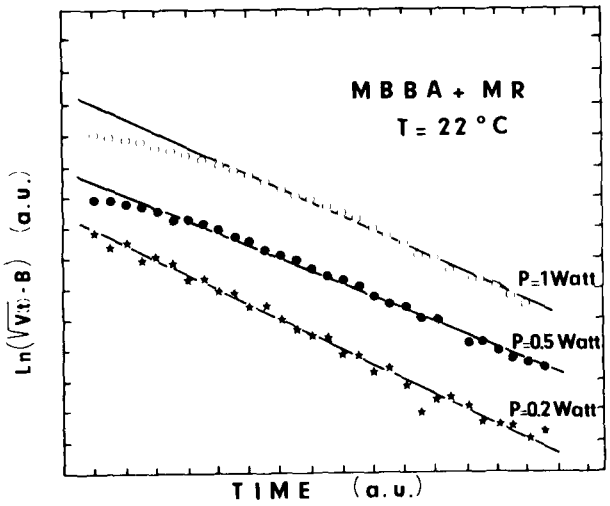

FIG. 3. Semilog plot of the square root of the phototube output voltage (minus the constant background B) vs the elapsed time following the initial sample photoexcitation. The three curves correspond to various values of the excitation Ar^+ laser power for a MR-doped MBBA sample.

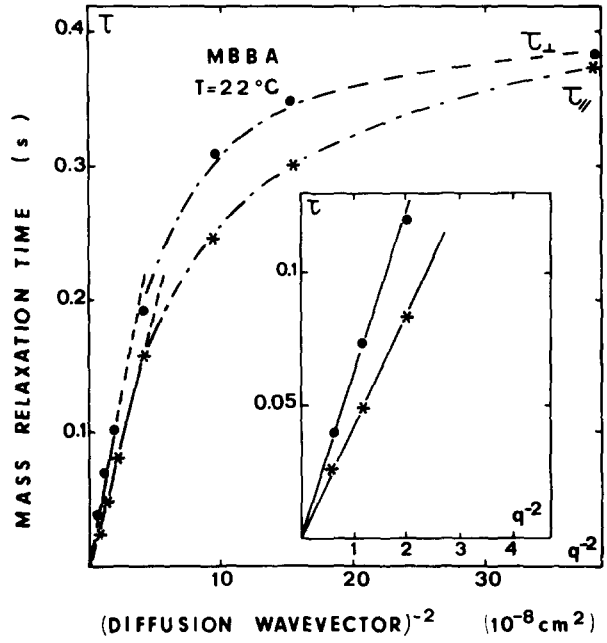

FIG. 4. Decay time of the diffracted light intensity vs the inverse square of the grating wave vector for parallel ($\tau_\parallel$) and perpendicular ($\tau_\perp$) geometries. The experimental points corresponding to low q^{-2} values have been blow up in the inset. Sample is undoped MBBA. The diffusing species are photoactivated MBBA molecules.

The sample thickness was typically 100 μm. In the case of the UV irradiation for pure PAA and MBBA samples, the molar absorptivity at 350 nm is so high ($\epsilon \simeq 1 - 2\times 10^4$ ℓmol^{-1} cm^{-1} [19]) that all the incident radiation is adsorbed in the first few μ. Therefore the photogenerated species are initially located in a small volume next to the entrance glass plate. Their concentration profile along the direction of the propagating beam is almost point-like. With MR-doped samples, on the contrary, the concentration of the dye impurity is adjusted so that only 50% of the incident light excitation (514.5 nm) is absorbed. The concentration of photogenerated species in the direction of the propagating beam is therefore much more uniform. Fortunately, this difference does not affect our results which can both be treated in the same way, since the FRS method automatically selects one component of the Fourier transform of the diffusion equation.

IV. RESULTS

For simplicity, in this section, we will use $D_\parallel$ and $D_\perp$ instead of $\tilde{D}^2_{S\parallel}$ and $\tilde{D}^2_{S\perp}$ or $\tilde{D}^3_{A\parallel}$ $\tilde{D}^3_{A\perp}$ and according to whether we are studying the two- or three-component cases.

Figure 4 displays the measured relaxation time τ of the diffraction grating vs the inverse square of the grating wave vector q^{-2} for pure MBBA samples. At low q^{-2} values (see inset), the data points for the two fringe orientations relative to the sample alignment axis fall on two straight lines passing through the origin. $\tau_\parallel$ and $\tau_\perp$ are thus proportional to the square of the fringe spacing, as expected for purely diffusive processes. At large q^{-2} values, however, both $\tau_\parallel$ and $\tau_\perp$ level off to a constant value, independent of the experimental geometry. This is consistent with the idea that for large fringe spacings, the intramolecular relaxation time becomes dominant over the relaxation time by mass diffusion. Consequently the data of Fig. 4 must then be fitted with Eq. (4).

We get

$$D_\parallel = (2.43 \pm 0.15)\ 10^{-7}\ \text{cm}^2\ \text{s}^{-1},$$
$$D_\perp = (1.61 \pm 0.16)\ 10^{-7}\ \text{cm}^2\ \text{s}^{-1},$$
$$\tau_R = 0.60 \pm 0.13\ \text{s}.$$

Figures 5(a) and 5(b) show the corresponding data for MBBA samples containing photoactivated MR molecules. The experimental points in the two different geometries align on two straight lines passing through the origin. The associated diffusion coefficients are

$$D_\parallel = (1.47 \pm 0.12)\ 10^{-7}\ \text{cm}^2\ \text{s}^{-1},$$
$$D_\perp = (0.88 \pm 0.06)\ 10^{-7}\ \text{cm}^2\ \text{s}^{-1}.$$

Here we observe no evidence of saturation at the largest q^{-2} values investigated, which correspond to diffusion lengths of 90 μm [see Fig. 5(b)]. It appears that the intramolecular relaxation time of MR is long compared to the mass diffusion time. Therefore, there is no contribution other than mass transport to the decay of the diffraction pattern. To confirm this point, we have measured the intramolecular relaxation time of MR in a conventional Cary 219 spectrophotometer following a spatially uniform excitation of the sample. From the data of Fig. 6, τ_R was found to be

$$\tau_R = 64 \pm 1\ \text{s}.$$

It should be remarked that the $D_\parallel$ and $D_\perp$ values reported here are smaller by a factor of 1.4 than indicated in Ref. 12. The origin of this discrepancy has to do with the amount of He–Ne laser light incident on the sample. In our previous experiment, it was much too large (8×10^{-5} W) and the intramolecular relaxation time of photoexcited MR molecules was considerably shortened, becoming comparable to the mass diffusion time. The more complete Eq. (4) has therefore to be used. Reanalyzing the data of Ref. 12, we obtain

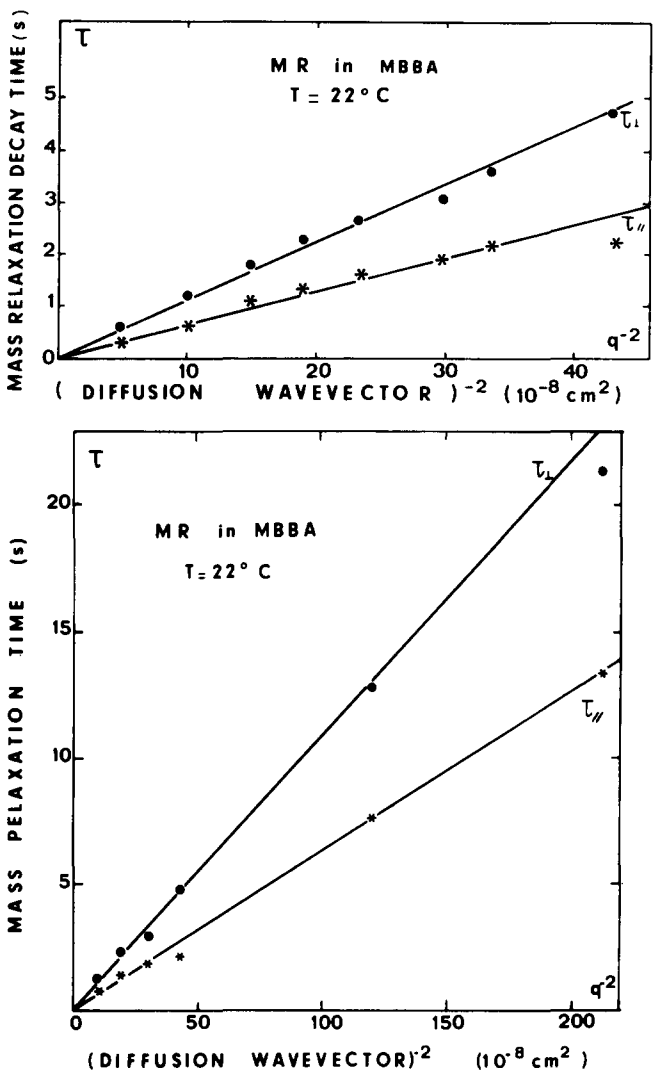

FIG. 5. Same as Fig. 4 but for photoactivated methyl red molecules dissolved in MBBA. (a) Data points obtained at low q^{-2} values; (b) data points obtained up to the highest q^{-2} values experimentally obtainable.

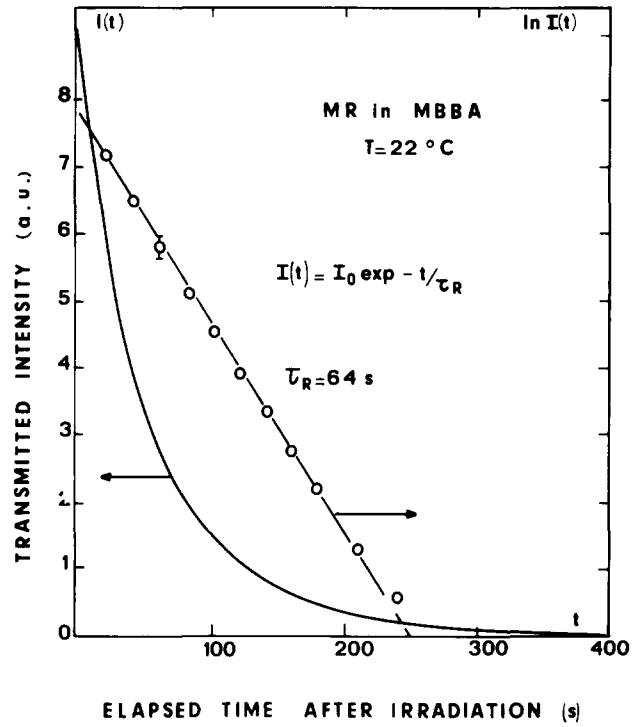

FIG. 6. Left-hand scale: time variation of the light intensity transmitted through a sample of photoactivated methyl red molecules in MBBA. Excitation is spatially uniform. Measurement is by a Cary 219 UV-VIS spectrometer used at 530 nm. The decrease is due to the *cis→trans* intramolecular relaxation process. Right-hand scale: same data in semilog coordinates. The slope yields the thermal (dark) relaxation time of MR in MBBA: $\tau_R = 64 \pm 1$ s.

$D_\parallel = (1.7 \pm 0.2) \times 10^{-7}$ cm^2 s^{-1}, $D_\perp = (0.98 \pm 0.12) \times 10^{-7}$ cm^2 s^{-1}, and $\tau_R = 4$ s, in good agreement with the present results.

We have systematically investigated the effect of visible light illumination on the grating relaxation in the case of MR-doped MBBA samples. In Fig. 7 we have plotted the relaxation time τ of the diffraction grating as a function of the inverse of the incident red laser power P_R, for a fixed grating vector of 6×10^{-4} cm^{-1}. We observe that τ is not a constant. It decreases rapidly with P_R^{-1} and reaches a plateau only for power levels below 5×10^{-6} W. This is clear evidence that too large power levels of the reading red laser can indeed deactivate the MR molecules from their *cis* state. The dashed curve in Fig. 7 corresponds to the *cis–trans* intramolecular relaxation time τ_R as deduced from fitting Eq. (20) to the data points and using Eq. (4) for the time constant. τ_R can be as low as 1 s for red light levels of the order of 5×10^{-3} W and reaches its thermal dark relaxation value of 64 s for levels below 5×10^{-6} W.

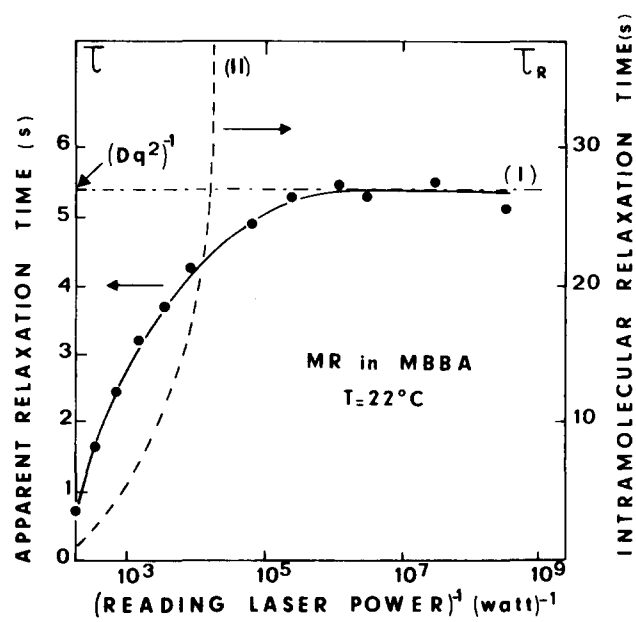

FIG. 7. Left-hand scale: apparent relaxation time τ of the light intensity diffracted in the first order vs the inverse power of the He–Ne continuous reading laser P_R^{-1}. At high P_r^{-1} values, τ saturates and tends towards a constant value $= (Dq^2)^{-1}$. The grating wave vector is fixed at 6×10^{-4} cm^{-1}. Right-hand scale: apparent relaxation time of photoexcited methyl red molecules vs P_R^{-1}, as calculated from Eq. 4. At high P_r^{-1}, this photoactivated relaxation time tends towards the thermal intramolecular relaxation value of 64 s.

We have repeated the same series of mass diffusion experiments for pure PAA samples. Figure 8 shows the relaxation time of the diffraction grating as a function of the inverse square of the grating wave vector. The data points for a given orientation can be fitted to a straight line over the whole range of grating spacings. Contrary to the case of photoexcited MBBA molecules, there is no evidence of saturation at the largest grating spacings. From the slopes of the two curves corresponding to the parallel and perpendicular orientation, respectively, we obtain

$$D_{\parallel} = 4.35 \pm 0.3 \times 10^{-6}\ \text{cm}^2\ \text{s}^{-1},$$

$$D_{\perp} = 3.1 \pm 0.3 \times 10^{-6}\ \text{cm}^2\ \text{s}^{-1}.$$

The temperature of the experiment was 126 °C. Note that the uncertainty of the data points is fairly large. This is due to the poor signal-to-noise ratio attainable with pure PAA samples, at least with a red reading laser. We have not attempted to see if a different wavelength could help to maximize the light intensity diffracted by the photoinduced grating. This was partially compensated by keeping the pulsed light excitation to a high level (1.2 W).

Figure 9 show the results for PAA samples doped with MR. From the slopes of the straight lines, we deduce

$$D_{\parallel} = 2.1 \pm 0.1 \times 10^{-6}\ \text{cm}^2\ \text{s}^{-1},$$

$$D_{\perp} = 1.45 \pm 0.1 \times 10^{-6}\ \text{cm}^2\ \text{s}^{-1},$$

at a temperature of 126 °C.

Note that only a restricted range of q^{-2} has been used. This is due to the fact that the intramolecular relaxation time of MR becomes small at elevated temperatures.

V. DISCUSSION

We shall start by examining the diffusion coefficients obtained by FRS for the pure (undoped) samples.

The best accepted values for the self-diffusion of PAA in the parallel and perpendicular geometries are those of Yun and Fredrickson[3] using radioactive labeled PAA: $D_{\parallel} = 4 \times 10^{-6}$ cm^2 s^{-1} and $D_{\perp} = 3.2 \times 10^{-6}$ cm^2 s^{-1} at 125 °C. They were later rather well confirmed by Töpler *et al.*[9] using high resolution quasielastic neutron scattering.

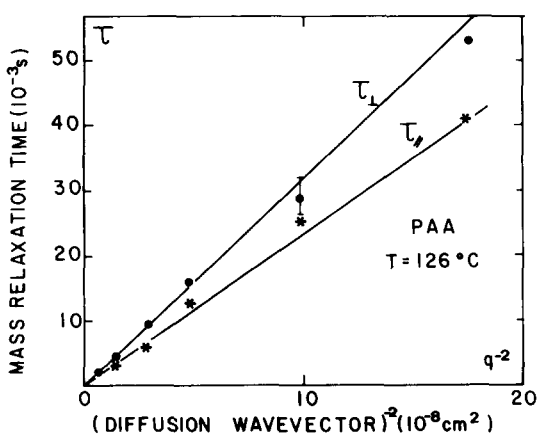

FIG. 8. Decay time of the diffracted light intensity vs the inverse square of the grating wave vector for parallel ($\tau_{\parallel}$) and perpendicular ($\tau_{\perp}$) geometries. Sample is undoped PAA. The diffusing species are photoactivated PAA molecules.

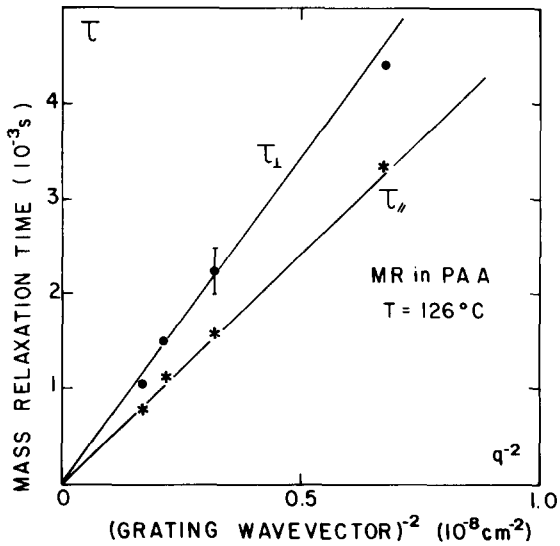

FIG. 9. Same as Fig. 8 but for photoactivated methyl red molecules dissolved in PAA.

These authors propose $D_{\perp} = 3.4 \pm 0.2 \times 10^{-6}$ cm^2 s^{-1} and $\bar{D} = D_{\parallel} + 2D_{\perp}/3 = 4.1 \pm 0.3 \times 10^{-6}$ cm^2 s^{-1} from which $D_{\parallel}$ can be easily calculated to be 5.5×10^{-6} cm^2 s^{-1}. Here we obtain by FRS $D_{\parallel} = 4.35 \pm 0.3 \times 10^{-6}$ cm^2 s^{-1} and $D_{\perp} = 3.1 \pm 0.3 \times 10^{-6}$ cm^2 s^{-1} for PAA at 126 °C.

To the best of our knowledge there are no self-diffusion data for MBBA. It is true that one experiment has been performed by multiple-pulse NMR on deuterated MBBA.[20] However, these data are very doubtful since even the sign of the diffusion anisotropy is not respected, i.e., $D_{\parallel}$ was found to be smaller than $D_{\perp}$. Until now, the closest approach to self-diffusion in MBBA remains the study of the diffusion of colored dyes in well-aligned samples. In one experiment,[4] the spreading of methyl red molecules injected through a precision-drilled hole was followed by optical densitometry. It was shown that $D_{\parallel} = 2.6 \times 10^{-6}$ cm^2 s^{-1} and $D_{\perp} = 1.6 \times 10^{-6}$ cm^2 s^{-1} at 22 °C. Since the molecular structure of methyl red is akin to that of MBBA, these diffusion coefficients are probably close to those of the matrix molecules. A further check of these data is provided by Hakemi and Labes[5] in their measurements of diffusion of phenyl-4-benzoxy benzoate in MBBA. Following the Cohen–Turnbull rule for the diffusion of tracers with arbitrary molecular shapes in liquids,[21] they assumed that the measured diffusion coefficient was inversely proportional to the mass of the diffusant. Using the relation

$$D_{\text{tracer}}/D_{\text{MBBA}} = (M_{\text{MBBA}}/M_{\text{tracer}})^{1/2},$$

and after correcting for an initial error, they got $D_{\parallel} = 2.7 \pm 10^{-7}$ cm^2 s^{-1} and $D_{\perp} = 1.3 \times 10^{-7}$ cm^2 s^{-1} for MBBA at 22 °C. These values are certainly in the range of the data cited above. On the contrary, they do not support data by a third group on the MR–MBBA system which seems to be three times too low.[22] It is true, however, that the Cohen–Turnbull rule is not obeyed in all systems[1] and this point should be further investigated. In the present experiments using FRS, we obtain

$$D_{\parallel}(\text{FRS}) = 2.43 \pm 0.15 \times 10^{-7}\ \text{cm}^2\ \text{s}^{-1}$$

and

$$D_{\perp}(\text{FRS}) = 1.61 \pm 0.16 \times 10^{-7}\ \text{cm}^2\ \text{s}^{-1}$$

for MBBA at 22 °C.

On the whole, the comparison between the data obtained by FRS in pure (undoped) samples and those obtained earlier by tracer techniques show a very close agreement for both PAA and MBBA. We can thus draw the conclusion that FRS measures the true self-diffusion coefficient when the photoactivated species are the molecules of the matrix itself. This is in accordance with the fact that the structural changes between the ground state and the photoactivated state are relatively minor for both molecules. Therefore one can assume in Eq. (15) that $D^0_{S^*} \cong D^0_S$. Moreover, the excitation level for inducing the transient grating has been kept low enough so the volume fraction of photoactivated species Φ_{S^*} is much less than one. On the whole, the correction terms are negligible and Eq. (15) reduces to $\tilde{D}^2_{S^*} \cong D^0_S$.

If we now turn to the results obtained by FRS on MR-doped samples, we immediately notice a large difference from the results obtained on the pure samples which have just been discussed. Indeed, there is roughly a factor of 2 between the two sets of data. At first sight, this may not look too surprising since Eqs. (15) and (19) tell us that the diffusion coefficients measured by FRS should not be identical in the case of a two- and a three-component system, i.e., $\tilde{D}^2_{S^*} \neq \tilde{D}^3_{A^*}$. The discrepancy, however, seems anomalously large. As explained in Sec. II B 3, the correction terms to the self-diffusion coefficient should become significant only if the interaction parameters between the various components of the fluid mixture assume very high values. We have therefore looked for a possible spurious association between the dye molecules following photoactivation, which would decrease the observed value of the diffusion coefficient.

Methyl red molecules are acids with a carboxylic group and can therefore be involved in hydrogen bonding. To test this possibility, we have performed additional FRS experiments with the ester form of methyl red, i.e., methyl red methyl ester (MRME), which is incapable of hydrogen bonds. Notwithstanding, the FRS values for the diffusion of MRME in MBBA are found to be identical to those obtained for methyl red, namely $D_{\parallel} = 1.5 \pm 0.15 \times 10^{-7}\ \text{cm}^2\ \text{s}^{-1}$ and $D_{\perp} = 1.0 \pm 0.15 \times 10^{-7}\ \text{cm}^2\ \text{s}^{-1}$ at 22 °C.

Another force which could drive intermolecular association is dipole–dipole interaction. We have already mentioned that, upon UV photoexcitation, the azobenzene moiety of methyl red isomerizes from the *trans* to the *cis* isomer. The two forms have very different dipole moments.[23] *Trans*-azobenzene has a low apparent dipole moment of 0.52 D. This is due to the fact that the molecule has a center of symmetry and the residual dipole moment is only due to distortion polarization. On the contrary, *cis*-azobenzene has a large dipole moment of 3.08 D due to its highly kinked structure. It is possible that this large dipole could favor intermolecular associations in the photoactivated state. This in turn would decrease the measured diffusion coefficient. Such an explanation, although difficult to prove directly, would have the additional advantage of explaining several independent observations. First, the diffusion of methyl red molecules in the absence of UV photoexcitation, as in the case of tracer diffusion of Ref. 4, does not yield anomalously low diffusion coefficient values. Second, we have already mentioned that at high volume fraction of photoactivated MR (corresponding to large excitation levels), the relaxation of the grating observed by FRS becomes nonlinear. Third, self-amplifying diffraction grating signals can be observed in samples doped with a high (1%) concentration of MR. All these points are consistent with our hypothesis of dye aggregation between MR molecules in their *cis* state and the fact that, on the contrary, they do not aggregate in their *trans* configuration. It is interesting to note in this context that Irie has recently reported another example of photoinduced demixing in polymeric systems bearing azobenzene chromophores.[24]

After these experiments were completed, we became aware of FRS results by Takezoe *et al.*[25] on the same MR-doped MBBA system. They also observe diffusion coefficients which are too low compared to the tracer data. We tentatively suggest that, as in our case, this is due to dye aggregation (their $D_{\parallel}$ and $D_{\perp}$ MR data are even lower than ours, which could be explained by a higher degree of interaction).

VI. COMPARISON WITH FRANKLIN THEORY OF DIFFUSION IN LIQUID CRYSTALS

By analogy with the Kirkwood–Riseman theory of mass diffusion in polymer solutions,[26] Franklin[27] has established the theoretical expressions for the two components of the mass diffusivity, $D_{\parallel}$ and $D_{\perp}$, in liquid crystals:

$$D_{\parallel} = kT\left[(\mu f_{\parallel})^{-1} + \frac{2+S}{6\pi\mu^2\Phi\alpha_{\parallel}}\right],$$
$$D_{\perp} = kT\left[(\mu f_{\perp})^{-1} + \frac{5-S}{12\pi\mu^2\Delta\alpha_{\perp}}\right] \tag{22}$$

where

$$\mu = \Sigma_1 (b_1/b)^2, \quad \Phi^{-1} = \sum_{1 \neq s} |R_{1s}|^{-1}.$$

b is the average of the two minor axes of the molecule while b_1 is the length of the segment 1 projected onto the long molecular axis (see Fig. 1).

R_{1s} is the vector distance between the molecular segments 1 and s.

The actual Φ^{-1} and μ values for PAA, MBBA, and MR have been calculated from molecular models and are indicated in Table I. $f_{\parallel}$ and $f_{\perp}$ have the dimensions of a friction coefficient but, unfortunately, are not calculable directly. Franklin has made the supplementary assumption of an isotropic friction factor, namely $f_{\parallel} = f_{\perp} = f$.

S is the usual orientational order parameter which describes the degree of alignment of the long molecular axes relative to the local optical axis, typically $S \simeq 0.6$.[28]

α describes the viscosity tensor for nematic liquid crystals.

$\alpha_{\parallel}$ and $\alpha_{\perp}$ are two particular combinations of the five independent viscosity coefficients first introduced by Ericksen and Leslie.[29,30]

$$\alpha_{\parallel} = 4\alpha_1 + \tfrac{1}{2}\alpha_2 + \tfrac{11}{2}\alpha_3 + 2\alpha_4 + 6\alpha_5,$$
$$\alpha_{\perp} = -\tfrac{13}{2}\alpha_2 + \tfrac{7}{4}\alpha_3 + 6\alpha_4 - \tfrac{3}{2}\alpha_5.$$

Note that these expressions for $\alpha_{\parallel}$ and $\alpha_{\perp}$ are not quite identical to the Franklin derivation due to some misprints in his original paper. The numerical values are $\alpha_{\parallel} = 425\times10^{-2}$ P and $\alpha_{\perp} = 931\times10^{-2}$ P in the case of MBBA,[27] and $\alpha_{\parallel} = 41.9\times10^{-2}$ P and $\alpha_{\perp} = 65.8\times10^{-2}$ P in the case of PAA.[31] In the following, we shall assume that they are not significantly affected by the addition of small amounts of methyl red dye.

Using Eqs. (22), we have first calculated the difference $(D_{\parallel} - D_{\perp})_{\text{theor}}$. In the Franklin model, this quantity is independent of the friction factor f. The data in columns 7 and 8 of Table I show that the agreement with the experimental value $(D_{\parallel} - D_{\perp})_{\text{expt}}$ is better than 20% for MBBA and MR and slightly worse for PAA. Using the experimental values of $D_{\parallel}$ and $D_{\perp}$, Eqs. (22) yield directly $f_{\parallel}$ and $f_{\perp}$. The values are reported in columns 9 and 10. They are very close to each other, which justifies the Franklin assumption of an isotropic friction for elementary segments. Taking an average $(f_{\parallel} + f_{\perp})/2$ for f, we can now calculate the absolute values for $D_{\parallel}$ and $D_{\perp}$ in the Franklin model. Examination of columns 5–12 and 6–13 in Table I shows that the correspondence with the experimental data for the two components of the diffusion tensor is very satisfying.

Despite its apparent success in explaining our observations, it should, however, be borne in mind that Franklin's theory is based on an analogy with polymer rheology in which the number of segments is large. This is clearly not the case for liquid crystals and the agreement may thus be fortuitous. It would be interesting to consider cases where the difference $D_{\parallel} - D_{\perp}$ inverts its sign with decreasing temperatures, as in the nematic phase of *p*-benzilidene-*p*-*n*-butyloxy aniline.[2] Such cases, which are frequently encountered in the vicinity of phase transitions to smectic ordering, should provide a critical check of Franklin's theory.

For the sake of completeness, we will also mention the theoretical calculations of Chu and Moroi.[32] They have derived the mass diffusion coefficients by using a properly parametrized form of the velocity autocorrelation function. Two coupled equations were proposed for $D_{\parallel}$ and $D_{\perp}$:

$$D_{\parallel} = \overline{D}\left[1 + \frac{2(1-\gamma)S}{2\gamma + L}\right],$$
$$D_{\perp} = \overline{D}\left[1 + \frac{(1-\gamma)S}{2\gamma + L}\right], \tag{23}$$

where $\gamma = \pi d/4L$ is a geometrical factor for rod-like molecules of length L and diameter d, S is the order parameter and $\overline{D}$ is the average diffusion coefficient:

$$\overline{D} = 1/3(D_{\parallel} + 2D_{\perp}).$$

To compare these theoretical expressions to the experimental values for the diffusion coefficients, it is convenient to use the ratio $D_{\parallel}/D_{\perp}$ since, in that case, $\overline{D}$ is automatically canceled out. For MBBA, $L \simeq 19$ Å and $d \simeq 5$ Å and therefore $\gamma = 0.21$; S is of the order of 0.6 at room temperature. Equations (23) then yield a theoretical value for $D_{\parallel}/D_{\perp}$ equals 2.49. This data disagrees with the experimental value of 1.5.

TABLE I. Comparison of experimental self-diffusion coefficient data with Franklin's theory for *p*-methoxy benzilidene *p*-*n* butyl aniline (MBBA), methyl red (MR), and *p*-azoxy anisol (PAA). b, μ, and ϕ have been calculated according to their definition in the text.

Compound name	b (10^{-8} cm)	μ	ϕ (10^{-9} cm)	$D_{\parallel\text{expt}}$ (10^{-7} cm^2/s)	$D_{\perp\text{expt}}$ (10^{-7} cm^2/s)	$(D_{\parallel} - D_{\perp})_{\text{expt}}$ (10^{-7} cm^2/s)	$(D_{\parallel} - D_{\perp})_{\text{theor}}$ (10^{-7} cm^2/s)	$f_{\parallel}$ (10^{-8} P cm)	$f_{\perp}$ (10^{-8} P cm)	$\langle f \rangle$ (10^{-8} P cm)	$D_{\parallel\text{theor}}$ (10^{-7} cm^2/s)	$D_{\perp\text{theor}}$ (10^{-7} cm^2/s)
MBBA												
This work $T = 22$ °C	5	3.15	1.41	2.4	1.68	0.72	0.58	8.9	9.8	9.4	2.33	1.75
MR												
Ref. 4 $T = 22$ °C	6	2.35	1.55	2.6	1.56	1.04	0.95	16.4	18	17.2	2.55	1.60
PAA												
This work $T = 126$ °C	5.15	2.95	1.47	43.5	31	12.5	6.54	0.64	0.80	0.72	40.2	33.6

A similar discrepancy is also observed for PAA. Therefore the Chu–Moroi calculations do not seem to provide a good description of our experimental data.

VII. CONCLUSION

The present experiments show that FRS is a powerful and precise method for measuring mass diffusion coefficients in fluid systems. If the molecules of the matrix are photosensitive, one has access to the true self-diffusion coefficient, provided the photoactivated state is not drastically different from the ground state. The present results obtained for *p*-azoxy anisol and *p*-methoxy benzilidene-*p*-*n*-butyl aniline are in agreement with the existing data derived from radioactive tracer and quasielastic neutron scattering measurements. If the molecules of the matrix are not photosensitive, extrinsic photochromic molecules must be dissolved in the sample. We have shown theoretically that FRS then measures a different diffusion coefficient. The experimental results obtained from PAA and MBBA samples doped with methyl red seem to confirm this point. However, we feel that the difference is too large to be explained by regular interactions between the components of the fluid mixture. In the particular case of methyl red we suspect the existence of specific intermolecular interactions in the photoactivated state. Formation of small aggregates could indeed slow down the diffusion process by a factor of 2. Such a hypothesis is difficult to test directly but it is striking that it would also explain several independent observations.

The present experiments emphasize the fact that the photochemical labeling required by FRS is not as innocuous as the nuclear labeling required by the more classical tracer techniques. Great care must then be exercised in the selection of the diffusing probes to avoid spurious intermolecular interactions.

Last, we have compared self-diffusion data in pure MBBA and PAA samples with the predictions of Franklin and of Chu and Moroi. We find a much better agreement in the first case.

ACKNOWLEDGMENTS

The MBBA was kindly supplied to us by L. Strzelecki and L. Liebert. The SiO- evaporated plates used to obtain oriented nematic samples were prepared by Mrs. Boix at the Université de Paris-Sud, Orsay. We also acknowledge helpful discussions with J. F. Joanny on the theoretical aspects of this problem.

APPENDIX: MUTUAL DIFFUSION IN THE CASE OF A THREE-COMPONENT MIXTURE

Let us consider a fluid mixture of solvent molecules S and dye molecules which can exist in two different states, A and A^*. The corresponding volume fractions are called ϕ_i with $i = A, A^*$, or S. One has the supplementary condition that $\Sigma_i \phi_i = 1$.

The free energy of the system can be written as

$$F = kT\left(\sum_i \phi_i \ln \phi_i + \frac{1}{2}\sum_j \sum_{i\neq j} \chi_{ij}\phi_i\phi_j\right), \tag{A1}$$

where $kT\chi_{ij}$ is the excess free energy of mixing between species i and j. The chemical potentials μ_i and the currents J_i are, respectively,

$$\mu_i = kT\left(\ln \phi_i + \sum_{j\neq i} \chi_{ij}\phi_J\right) + \text{const} \tag{A2}$$

and

$$J_i = -\Lambda_i \nabla(\mu_i + U), \tag{A3}$$

where U as in Sec. II B, is a potential which accounts for the incompressibility of the system. By imposing the conservation of fluxes, i.e., $\Sigma J_i = 0$, U is calculated to be

$$U = -\sum_i \Lambda_i \mu_i \Big/ \sum_i \Lambda_i. \tag{A4}$$

Restricting our attention to the A^* current we obtain

$$J_{A^*} = -\Lambda\left[(\Lambda_A + \Lambda_S)\nabla(\mu_{A^*} - \mu_S) - \Lambda_A \nabla(\mu_A - \mu_S)\right] \tag{A5}$$

with

$$\Lambda = \Lambda_{A^*} \Big/ \sum_i \Lambda_i. \tag{A6}$$

Note that the A^* current depends only upon the exchange potentials $(\mu_{A^*} - \mu_S)$ and $(\mu_A - \mu_S)$.

Using the expressions (A2) for the μ_i's we get

$$J_{A^*} = -D_{A^*A^*}\nabla\phi_{A^*} - D_{A^*A}\nabla\phi_A - D_{A^*S}\nabla\phi_S, \tag{A7}$$

where

$$\begin{aligned} D_{A^*A^*} &= \Lambda\left[\Lambda_A(1/\phi_{A^*} - \chi_{AA^*}) + \Lambda_S(1/\phi_{A^*} - \chi_{A^*S}\right], \\ D_{A^*A} &= \Lambda\left[\Lambda_A(\chi_{AA^*} - 1/\phi_A) + \Lambda_S(\chi_{AA^*} - 1/\phi_S)\right], \\ D_{A^*S} &= \Lambda\left[\Lambda_A(\chi_{A^*S} - \chi_{AS}) + \Lambda_S(\chi_{A^*S} - 1/\phi_S)\right]. \end{aligned} \tag{A8}$$

Since $\Sigma_i \phi_i = 0$, $\nabla\phi_S$ can be replaced by $-(\nabla\phi_A + \nabla\phi_{A^*})$ and J_{A^*} becomes

$$J_{A^*} = -\tilde{D}_{A^*A^*}\nabla\phi_{A^*} - \tilde{D}_{A^*A}\nabla\phi_A \tag{A9}$$

with

$$\tilde{D}_{A^*A^*} = \Lambda\left[\Lambda_{A^*}\left(\frac{1}{\phi_{A^*}} - \chi_{AA^*} - \chi_{A^*S} + \chi_{AS}\right) + \Lambda_S\left(\frac{1}{\phi_{A^*}} + \frac{1}{\phi_S} - 2\chi_{A^*S}\right)\right] \tag{A10}$$

and

$$\tilde{D}_{A^*A} = \Lambda\left[\Lambda_A(\chi_{AA^*} - 1/\phi_A - \chi_{A^*S} + \chi_{AS}) + \Lambda_S(\chi_{AA^*} - \chi_{A^*S})\right].$$

The Λ_i's are related to the D_i^0's, i.e., the mutual diffusion coefficients at infinite dilution of A and A^*, by

$$\Lambda_i = D_i^0\phi_i/kT. \tag{A11}$$

[1]See the recent review by G. J. Krüger, Phys. Rep. **82**, 229 (1982).
[2]A. Mircea-Roussel, L. Léger, F. Rondelez, and W. H. De Jeu, J. Phys. (Paris) Colloq. **36**, 93 (1975).
[3]C. K. Yun and A. G. Fredrickson, Mol. Cryst. Liq. Cryst. **12**, 73 (1970).
[4]F. Rondelez, Solid State Commun. **14**, 815 (1974).
[5]H. Hakemi and M. M. Labes, J. Chem. Phys. **63**, 3708 (1975). This paper corrects earlier results by the same authors and published in J. Chem. Phys. **61**, 4020 (1974).

[6]G. J. Krüger and H. Spiesecke, Z. Naturforsch. Teil A **28**, 964 (1973).
[7]R. Blinc, J. Pirš, and I. Zupančič, Phys. Rev. Lett. **30**, 546 (1973).
[8]V. Graf, F. Noack and M. Stohrer, Z. Naturforsch. Teil A **32**, 61 (1977).
[9]J. Töpler, B. Alefeld, and T. Springer, Mol. Cryst. Liq. Cryst. **26**, 297 (1974).
[10]A. J. Dianoux, A. Heidemann, F. Volino, and H. Hervet, Mol. Phys. **32**, 1521 (1976).
[11]See Ref. 1 of this paper and also G. Rollmann, K. F. Reinhart, and F. Noack, Z. Naturforsch. Teil A **34**, 964 (1979); F. Volino, A. J. Dianoux, and A. Heidemann, J. Phys. Lett. **40**, L-583 (1979).
[12]H. Hervet, W. Urbach, and F. Rondelez, J. Chem. Phys. **68**, 2725 (1978).
[13]H. Hervet, L. Léger, and F. Rondelez, Phys. Rev. Lett. **42**, 1681 (1979).
[14]D. L. Ross and J. Blanc, in *Photochromism*, edited by G.H. Brown, Vol. 3 in Techniques of Chemistry (Wiley, New York, 1971).
[15]D. R. Gaskell, in Physical Metallurgy, edited by R. W. Cahn and P. Haasen (North–Holland, Amsterdam, 1983), Vol. 1, p. 292.
[16]P. G. de Gennes, J. Chem. Phys. **72**, 4756 (1981).
[17]P. R. Bevington, *Data Reduction and Error Analysis for the Physical Sciences* (McGraw–Hill, New York, 1969).
[18]M. Tournarie, J. Phys. (Paris) **30**, 47 (1969).
[19]S. Chandrasekhar and N. V. Madhusudana, in *Applied Spectroscopy Reviews*, edited by E. G. Brame (Dekker, New York, 1973), Vol. 6, p. 189.
[20]I. Zupančič, J. Pirš, M. Luzar, R. Blinc, and J. W. Doane, Solid State Commun. **15**, 227 (1974).
[21]M. H. Cohen and D. Turnbull, J. Chem. Phys. **31**, 1164 (1959).
[22]H. Schulze and G. Schumann, Z. Phys. Chem. (Leipzig) **259**, 1037 (1978).
[23]D. J. W. Bullock, C. W. N. Cumper and A. I.Vogel, J. Chem. Soc. **1965**, 5316.
[24]M. Irie and H. Tanaka, Macromolecules **16**, 210 (1983).
[25]H. Takezoe, S. Ichikawa, A. Fukuda, and E. Kuze, Jpn. J. Appl. Phys. **23**, L78 (1983).
[26]J. G. Kirkwood, *Macromolecules* (Gordon and Breach, New York, 1967).
[27]W. Franklin, Phys. Rev. A **11**, 2156 (1975).
[28]P. G. de Gennes, *The Physics of Liquid Crystals* (Clarendon, Oxford, 1974).
[29]J. L. Ericksen, Arch. Ration. Mech. Anal. **4**, 231 (1960).
[30]F. M. Leslie, Q. J. Mech. Appl. Math. **19**, 357 (1966); Mech. Anal. **28**, 265 (1968).
[31]D. Langevin, Thèse d'Etat, Paris, 1974; L. Léger, Thèse 3ème cycle, Orsay, Paris, 1971; Orsay Liquid Crystal Group, Mol. Cryst. Liq. Cryst. **13**, 187 (1971).
[32]K. S. Chu and D. S. Moroi, J. Phys. (Paris) Colloq. **36**, 99 (1975).